J. Phys. B: Atom. Molec. Phys., Vol. 11, No. 11, 1978. Printed in Great Britain.

Electron impact excitation of magnesium at 10, 20 and 40 eV impact energies†

W Williams and S Trajmar
Jet Propulsion Laboratory, California Institute of Technology, Pasadena, California 91103, USA

Received 7 November 1977

Abstract. Normalised differential, integral and momentum-transfer cross sections for elastic scattering and for excitation of the 3^3P, 3^1P, 3^1D, 4^1S, 4^1P and ($3^3D + 3^3P$) states of magnesium have been determined at 10, 20 and 40 eV impact energies. Several autoionising transitions have been observed in the 8–12 eV region of the energy-loss spectra which correlate well with optical-absorption and ejected-electron spectra.

1. Introduction

Low-energy resonant scattering of electrons by magnesium was studied by Burrow and Comer (1975) using the electron transmission method. They reported a strong shape resonance at 0·15 eV. The electron impact excitation function for the 3^1P state was determined (by measuring the 2852 Å resonant radiation) by Aleksakhin *et al* (1973) and more recently by Leep and Gallagher (1976). Sphenik *et al* (1977) utilised a higher energy resolution in the electron beam and observed several sharp structures in the excitation function below 10 eV impact energy. No direct measurement of the elastic or inelastic electron scattering cross sections have been reported in the low and intermediate impact energy ranges.

Van Blerkom (1970) carried out calculations (semi-empirical potential, close-coupling method) for elastic scattering and for all possible transitions among the 3^1S, 3^3P and 3^1P states in the 0·14–8·16 eV range. A similar calculation was carried out by Fabrikant (1974) and produced substantial disagreement with Van Blerkom. Robb (1974) calculated the integral cross sections for the 3^1P excitation in the Born approximation from 10 to 2000 eV.

The oscillator strength for the 3^1P excitation has been measured by a number of investigators and their results summarised, for example, by Robb (1974) and Victor *et al* (1976).

The ejected-electron spectrum has been studied by Rassi *et al* (1977 and private communication) at electron impact energies of 17, 27, 40 and 500 eV and they compared the observed autoionisation structure to available calculations and photoionisation measurements. A summary of theoretical and photoionisation results can be found in the papers of Rassi *et al* (1977) and Mansfield and Connerade (1972).

† This paper presents the results of one phase of research carried out at the Jet Propulsion Laboratory, California Institute of Technology, under contract NAS7-100 sponsored by the National Aeronautics and Space Administration.

We report here differential, integral and momentum-transfer cross sections for elastic scattering and for excitation of the 3^3P, 3^1P and 3^1D states at 10, 20 and 40 eV impact energies. Cross sections for the 4^1S and 4^1P states are also reported at 20 and 40 eV and for the 3^3D and 4^3P (unresolved) states at 20 eV impact energies. Several autoionising features have been observed in the 8–12 eV energy-loss region.

2. Experimental

The measurements were performed with an electron impact spectrometer described previously by Chutjian (1974), Chutjian *et al* (1973) and Williams and Trajmar (1974). An electron beam (0·08 eV full width at half maximum) was scattered at right-angles by a magnesium beam (generated by heating a stainless-steel crucible to about 600 °C by electron bombardment). The magnesium vapour effused from a 0·1 cm diameter by 0·4 cm long channel to form the target beam. The beam intersection was 0·2 cm above the tip of the crucible. The unscattered electron beam was trapped and monitored with a Faraday cup.

The electron scattering intensities at fixed impact energies (E_0) and scattering angles (θ) were determined as functions of energy loss by pulse-counting and multichannel-scaling techniques. Repetitive scans were performed until the desired signal-to-noise ratio was reached. The angular resolution was around 2°. The impact energy scale is accurate to $\pm 0{\cdot}5$ eV. A typical energy-loss spectrum is shown in figure 1. From these spectra the relative inelastic scattering intensities were determined with respect to elastic scattering. The elastic scattering intensity was determined in a time which was short compared to instrumental drift. By applying an effective path-length correction appropriate for our scattering geometry (Williams *et al* 1976) differential cross sections (DCS) in arbitrary units were obtained from the elastic intensity measurements. Products of the inelastic/elastic intensity ratios and the elastic DCS yielded the inelastic DCS in the same arbitrary units. The cross sections were extrapolated to 0° and 180° scattering angles and then integrated to obtain integral and momentum-transfer cross sections. All cross sections were then normalised to the absolute scale by using the 3^1P excitation-function measurements of Leep and Gallagher (1976).

3. Results and discussion

3.1. Differential cross sections

A typical energy-loss spectrum at $E_0 = 25$ eV and scattering angle $\theta = 10°$ is shown in figure 1. Relative cross sections were determined from similar spectra in the 10–130° angular range at 10, 20 and 40 eV impact energies. Absolute cross sections were obtained by the method outlined above.

At low scattering angles an inelastic feature appeared at 8·70 eV (twice the energy-loss corresponding to the strong 3^1P excitation energy). No ejected electron corresponding to this energy loss was found and it has been suggested that it is due to double scattering (T W Ottley 1977 private communication). Our subsequent investigation of the relative intensities as a function of Mg pressure proved this to be the case and also showed that no other double-scattering feature was present in the spectrum. In all cases the $I(3^1P + 3^1P)/I(3^1P)$ ratio was less than 0·005. This

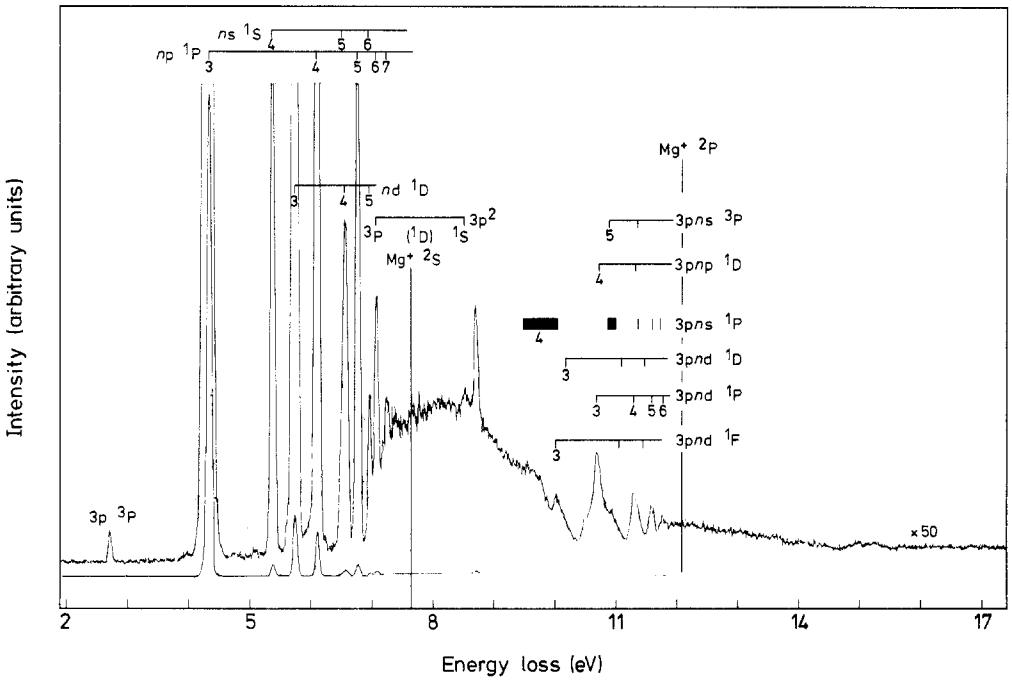

Figure 1. Energy-loss spectrum of Mg(...$2p^6 3s^2$ ^1S) at 25 eV impact energy and 10° scattering angle.

is a similar situation to the case of K discussed by Williams and Trajmar (1977) and we can conclude that neither the elastic nor the 3^1P excitation cross sections are significantly affected by double scattering.

The DCS are listed in tables 1–3 and are shown in figure 2. The elastic cross sections show the characteristic oscillations which we found previously in connection with other metals. The 3^1P excitation cross section is very strongly forward peaked, especially at the higher energies, and the magnitude of the DCS is comparable to the elastic scattering cross sections. This behaviour is again very similar to those found with other metals. The relative values of the cross sections are estimated to be accurate to about 30% except at angles below 20° where the cross sections rise very steeply. Further uncertainties are added to the absolute values because of the extrapolations from 10° to 0° and from 130° to 180° and because of the normalisation procedure. We estimate, however, that the absolute values are correct to within a factor of two.

For the normalisation of the cross section data we chose the 3^1P excitation function of Leep and Gallagher (1967) because the so-normalised data merges smoothly with the theoretical results of Fabrikant (1974) at low energies and because of the availability of this excitation function in tabular form. No experimental or theoretical differential cross sections are available to which the present results could be compared.

From the 20 and 40 eV 3^1P DCS, the apparent generalised oscillator strengths f_A^G were calculated using the equation

$$f_A^G(K^2) = \frac{W}{2}\frac{k_0}{k}K^2 \mathrm{DCS}(E,\theta)$$

Table 1. Differential cross sections (in units of 10^{-16} cm^2 sr^{-1}) at 10 eV impact energy. (The values in parentheses and at 0°, 140°, 160° and 180° were obtained by extrapolations.)

θ (deg)	Elastic	3^3P	3^1P	3^1D
0	56	1·6	27	0·38
10	(40)	0·90	17	0·23
20	23	0·51	9·9	0·16
30	9·7	0.36	4·2	0·12
40	2·9	0·40	2·0	0·10
50	0·70	0·51	1·2	0·090
60	0·16	0·44	0·68	0·070
70	0·026	0·33	0·33	0·055
80	0·21	0·27	0·23	0·042
90	0·55	0·22	0·16	0·032
100	0·60	0·15	0·13	0·025
110	0·60	0·10	0·12	0·022
120	0·58	0·084	0·11	0·022
130	0·54	0·076	0·12	0·027
140	0·49	0·071	0·12	0·033
160	0·41	0·064	0·13	0·051
180	0·33	0·058	0·15	0·077

where W is the excitation energy, k_0 and k are the momenta before and after scattering, and K^2 is the momentum transfer. The results are plotted in figure 3. Also shown in the figure are the generalised oscillator strengths calculated by Robb (1974) in the Born approximation. At the optical limit his value (1·82) agrees well with the experimental optical f value. The apparent generalised oscillator strengths calculated from the present cross sections are joined by full curves down to the 10° point.

Table 2. Differential cross sections (in units of 10^{-18} cm^2 sr^{-1}) at 20 eV impact energy. (The values in parentheses and at 0°, 140°, 160° and 180° were obtained by extrapolations.)

θ (deg)	Elastic	3^3P	3^1P	3^1D	4^1S	4^1P	3^3D + 4^3P
0	4400	0·83	19 000	400	66	330	7·8
10	(2400)	2·9	2700	270	37	180	9·2
20	1200	12	700	150	21	80	9·4
30	440	21	240	66	12	35	8·5
40	110	20	110	24	8·3	18	(6·4)
50	12	18	44	7·3	6·6	9·9	4·7
60	7·1	(12)	(26)	(6·4)	(4·6)	(6·2)	(3·7)
70	23	6·9	17	5·4	3·5	4·3	3·3
80	37	(1·9)	(13)	(1·9)	(2·5)	(1·8)	(0·9)
90	45	0·16	11	1·4	2·4	0·64	0·14
100	46	0·50	11	2·8	2·7	1·9	0·22
120	32	(1·1)	(11)	(3·1)	(2·8)	(2·4)	(0·29)
130	14	2·3	12	3·1	2·8	2·7	0·35
140	5·7	3·5	14	3·1	2·6	2·7	0·47
160	4·1	5·4	17	3·1	2·3	2·5	0·73
180	5·0	5·9	21	3·1	2·0	2·1	0·83

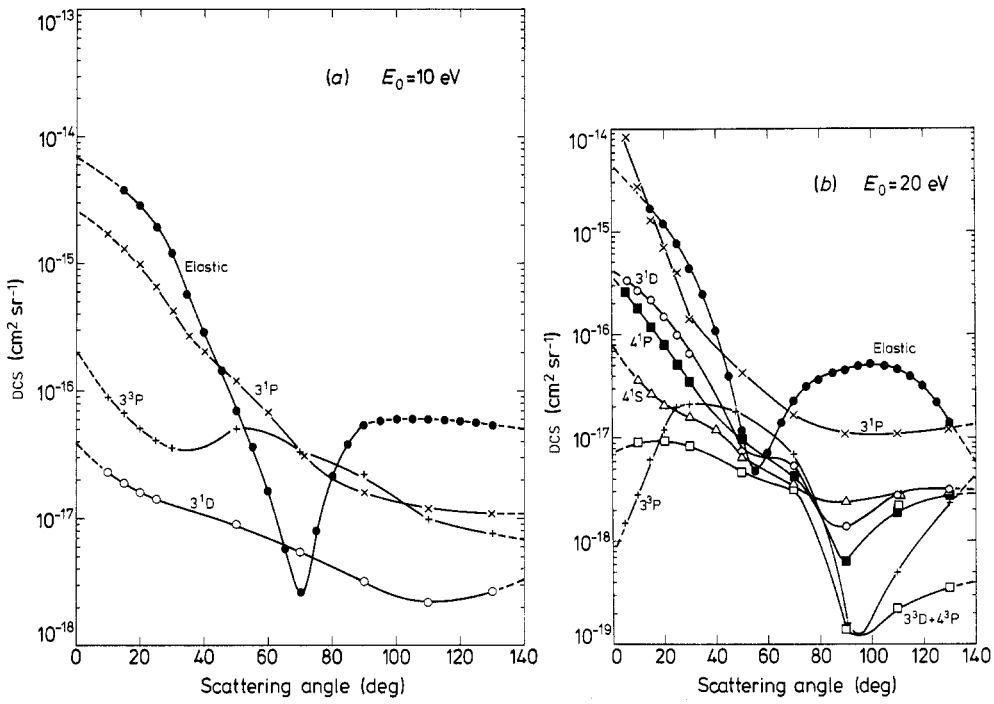

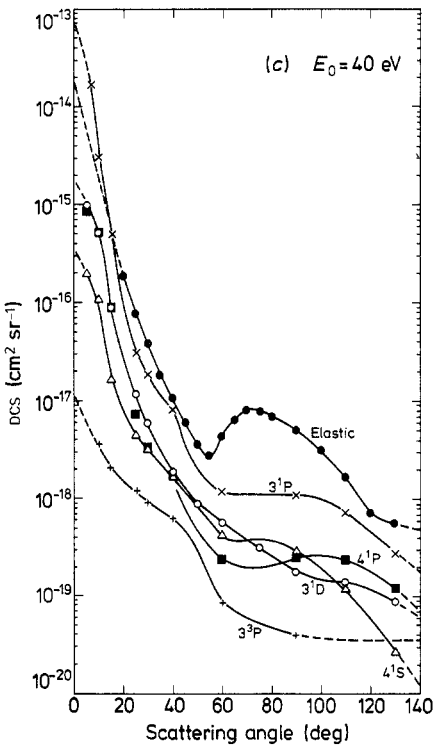

Figure 2. Differential cross sections at (*a*) 10 eV, (*b*) 20 eV, and (*c*) 40 eV.

Table 3. Differential cross sections (in units of 10^{-18} cm^2 sr^{-1}) at 40 eV impact energy. (The values in parentheses and at 0°, 140°, 160° and 180° were obtained by extrapolations.)

θ (deg)	Elastic	3^3P	3^1P	3^1D	4^1S	4^1P
0	17 000	12	71 000	1800	360	1400
10	(1800)	3·6	3100	540	110	540
20	190	1·5	88	26	7·1	16
30	39	0·93	19	6·1	3·3	3·5
40	11	0·64	8·2	1·9	1·7	1·8
50	3·7	0·31	(2·0)	0·90	0·82	0·68
60	4·5	0·087	1·2	0·58	0·43	0·42
75	8·0	0·054	1·1	0·32	0·40	0·24
80	7·0	(0·047)	(1·1)	(0·26)	(0·38)	(0·20)
90	5·1	0·020	1·1	0·18	0·34	0·25
100	3·2	(0·038)	(1·0)	(0·15)	(0·20)	(0·26)
110	1·7	0·036	0·72	0·14	0·12	0·24
120	0·72	(0·036)	(0·45)	(0·12)	(0·060)	(0·18)
130	0·57	0·036	0·27	0·087	0·027	0·12
140	0·49	0·036	0·17	0·060	0·013	0·075
160	0·36	0·036	0·087	0·030	0·0048	0·037
180	0·31	0·036	0·049	0·016	0·0022	0·020

Below this angle the 5° and 0° extrapolated DCS were used and the points are connected by broken curves. A more realistic extrapolation of the f_A^G values would be similar in shape to the low-momentum-transfer Born values. Such an extrapolation is shown by the dotted curve for the 50 eV case. It extrapolates to a somewhat higher value than the optical f value, which indicates that our cross sections are somewhat high due to cascade contributions in the excitation function which we used for normalisation.

3.2. Integral cross sections

The integral cross sections, obtained by extrapolation, integration and normalisation as described above, are listed in table 4 and shown in figure 4. Table 4 also contains the momentum-transfer cross sections. At 20 and 40 eV the 3^1P integral excitation cross section is comparable to or larger than the corresponding elastic cross section and the same applies to the respective momentum-transfer cross sections. This dominance of the resonance excitation process is typical for most of the metal atoms which we have studied and points again to the importance of inelastic momentum transfer in metal-vapour plasma systems.

The present elastic and 3^3P cross sections merge smoothly with the low-energy calculated cross sections of Fabrikant (1974) and so does the excitation function of Leep and Gallagher (1976) which served as a basis for our normalisation. Aleksakhin *et al* (1973) determined a 3^1P excitation function which is very similar to that of Leep and Gallagher, but lower by about a factor of two. Both of these excitation functions contain some cascade contributions and, therefore, represent an upper limit (as do our cross sections). The 3^1D, 4^1P and 4^1S integral excitation cross sections are also shown in figure 4, but not enough energy points are available to determine

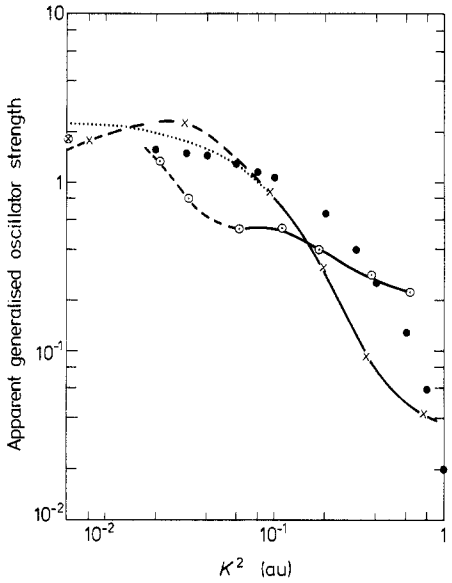

Figure 3. Generalised oscillator strengths as functions of the square of the momentum transfer calculated from the 40 eV (×) and 20 eV (⊙) DCS. The Born results of Robb (1974) (●) and the optical f value (⊗) are also shown. The dotted curve extrapolation of the 40 eV data follows the Born approximation-type extrapolation from the last reliably measured experimental point to zero momentum transfer.

their energy dependence reliably near the threshold region. The Born integral cross sections for the 3^1P excitation (Robb 1974) are higher than all other results.

3.3. The autoionisation region

In figure 1 the energy-loss spectrum extends beyond the first ionisation limit and reveals a number of structures associated with autoionising states. The 8·70 eV feature is due to double scattering as discussed above. The other features correlate well with the features observed in photoabsorption and ejected-electron spectra in general, but no detailed comparison can be made due to the low energy resolution of the present data. The autoionising states have been indicated on figure 1 by utilising the ejected-electron spectra of Rassi *et al* (1977), the photoabsorption measurements

Table 4. Integral (upper part) and momentum-transfer cross sections (lower part) (in units of 10^{-16} cm^2).

E_0	Elastic	3^3P	3^1P	3^1D	4^1S	4^1P	$3^3D + 4^3P$
10	29	3·1	14	0·7	—	—	—
20	16	0·8	15	2·1	0·6	1·3	3·0
40	6·6	0·03	14	1·3	0·3	1·2	—
10	7·6	2·1	5·9	0·5	—	—	—
20	4·1	0·5	3·9	0·8	0·4	0·6	1·5
40	0·47	0·009	1·0	0·14	0·5	0·14	—

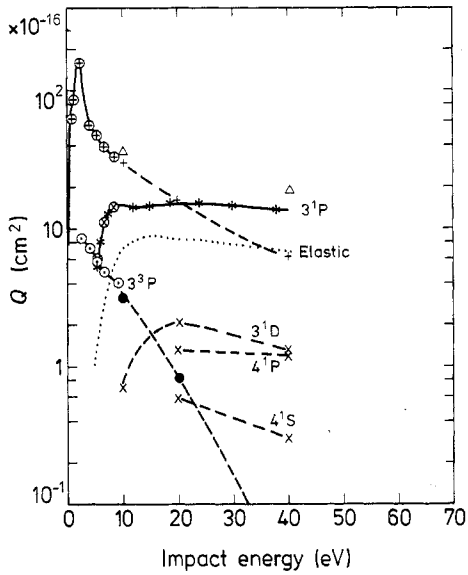

Figure 4. Integral cross sections: +, ×, ● present results; ⊕, ⊗, ⊙ Fabrikant (1974);* Leep and Gallagher (1976); ..... 3^1P excitation function of Aleksakhin *et al* (1973); △ 3^1P integral cross sections of Robb (1974).

of Mehlman-Balloffet and Esteva (1969), Esteva *et al* (1972) and Bradley *et al* (1975), and the theoretical results of Burke and Moores (1968), Laughlin and Victor (1972), Kulander and Dahler (1972), Bates and Altick (1973) and Thompson *et al* (1974).

Recent analysis of this region based on multichannel quantum-defect theory (Lu 1974, 1977 private communication) indicates a very strong mixing of the 3s*n*p ^1P and the 3s*n*d ^1D series and continua with the doubly excited 3p*n*s ^1P and $3p^2$ ^1D levels respectively, but no significant mixing of the 3s*n*s ^1S continuum and the $3p^2$ ^1S state. These interactions explain the very broad nature of the 3p*n*s ^1P excitation as well as the presence of the sharp feature for the $3p^2$ ^1S state. The analysis also requires the increase of the principal quantum number in the 3p*n*s ^1P series by one and places the $n = 4$ very broad state just above the first ionisation limit.

Acknowledgments

We would like to express our gratitude to Mr D Rassi, Mr V Pejčev, Dr T W Ottley and Dr K J Ross for sending us their results prior to publication.

References

Aleksakhin I S, Zapesochnyi I P, Garga I I and Starodub V P 1973 *Opt. Spectrosc.* **34** 611–5
Bates G N and Altick P L 1973 *J. Phys. B: Atom. Molec. Phys.* **6** 653–64
Bradley D J, Ewart P, Nicholas J V and Shaw J R D 1975 *J. Phys. B: Atom. Molec. Phys.* **8** 2934–8
Burke P G and Moores D L 1968 *J. Phys. B: Atom. Molec. Phys.* **1** 575–85
Burrow P D and Comer J 1975 *J. Phys. B: Atom. Molec. Phys.* **8** L92–5
Chutjian A 1974 *J. Chem. Phys.* **61** 4279–84
Chutjian A, Cartwright D C and Trajmar S 1973 *Phys. Rev. Lett.* **30** 195

Esteva J M, Mehlman-Balloffet G and Roman J 1972 *J. Quant. Spectrosc. Radiat. Transfer* **12** 1291–303
Fabrikant I I 1974 *J. Phys. B: Atom. Molec. Phys.* **7** 91–6
Kulander K C and Dahler J S 1972 *Phys. Rev.* A **6** 1436–51
Laughlin C and Victor G A 1972 *Atomic Physics 3, Proc. 3rd Int. Conf. on Atomic Physics* pp 247–55
Leep D and Gallagher A 1976 *Phys. Rev.* A **13** 148–55
Lu K T 1974 *J. Opt. Soc. Am.* **64** 706
Mansfield M W D and Connerade J P 1972 *Phys. Scr.* **6** 191–4
Mehlman-Balloffet G and Esteva J M 1969 *Astrophys. J.* **157** 945–56
Rassi D, Pejčev V, Ottley T W and Ross K J 1977 *J. Phys. B: Atom. Molec. Phys.* **10** 2913–21
Robb W D 1974 *J. Phys. B: Atom. Molec. Phys.* **7** 1006–17
Shpenik O B, Zapesochnyi I P, Sovter V V, Nepijpov E I, Romanjuk N I and Aleksakhin I S 1977 *Proc. 10th Int. Conf. on Physics of Electronic and Atomic Collisions* (Paris: Commissariat à l'Energie Atomique) Abstracts p 1302
Thompson D G, Hibbert A and Chandra N 1974 *J. Phys. B: Atom. Molec. Phys.* **7** 1298–305
Van Blerkom J K 1970 *J. Phys. B: Atom. Molec. Phys.* **3** 932–6
Victor G A, Stewart R F and Laughlin C 1976 *Astrophys. J. Suppl. Ser.* **31** 237–47
Williams W and Trajmar S 1974 *Phys. Rev. Lett.* **33** 187–90
——1977 *J. Phys. B: Atom. Molec. Phys.* **10** 1955–66
Williams W, Trajmar S and Bozinis D 1976 *J. Phys. B: Atom. Molec. Phys.* **9** 1529–36